# The Interaction of *Fusarium solani pisi* Cutinase with Long Chain Spin Label Esters†

Kristian R. Poulsen,‡ Thomas K. Sørensen,§,|| Laurent Duroux,‡ Evamaria I. Petersen,‡ Steffen B. Petersen,‡ and Reinhard Wimmer*,§

*Biostructure and Protein Engineering Group, Department of Physics and Nanotechnology, Aalborg University, DK-9220 Aalborg, Denmark, and Department of Life Sciences, Aalborg University, DK-9000 Aalborg, Denmark*

*Received February 16, 2006; Revised Manuscript Received May 26, 2006*

ABSTRACT: We here present a study of the interaction between the *Fusarium solani pisi* cutinase mutant S120A and spin-labeled 4,4-dimethyloxazoline-*N*-oxyl-(DOXYL)-stearoyl-glycerol substrates in a micellar system. The interaction is detected by NMR measuring changes in chemical shift for $^{1}$H and $^{15}$N as well as relaxation parameters for backbone $^{1}$H ($T_1$) and $^{15}$N ($T_1$, $T_2$) atoms as well as for side chain methyl groups $^{1}$H ($T_1$). The detected interaction shows a weak binding of cutinase to the lipid micelles. Structural and mobility changes are located inside and around the active site, its flanking loops, and the oxyanion hole, respectively. Relaxation changes in the amino acid pairs Ser 92, Ala 93 and Thr 173, Gly 174 positioned at the edge of each of the active site flanking loops make these residues prime candidates for hinges, allowing for structural rearrangement during substrate binding. The cutinase mutant S120A used carries a 15 amino acid pro-peptide; the significance of this pro-peptide was so far undetermined. We show here that the pro-peptide is affected by the presence of the micellar substrate. Relaxation enhancements indicative of spatial proximity between the DOXYL group in the lipid chain and some hydrophobic residues surrounding the active site could be found.

Cutinases are small lipolytic enzymes capable of hydrolyzing a vide variety of esters, including triglycerides of varying size. They show no interfacial activation above the CMC and are therefore not categorized as classical lipases but are placed as intermediates between lipases and esterases (*1*−*4*). *Fusarium solani pisi* cutinase is a member of the cutinase family (EC 3.1.1.74). Cutinase from *F. solani pisi* was first isolated from the extracellular fluid of the fungus where it showed activity toward cutin (*5*−*8*). Cutinase was sequenced first as cDNA (*9*) and later as gene with minor changes in the coding region (*10*).

The full-length cutinase gene codes for 230 amino acids (*9*). As the N-terminal amino acid of the native mature cutinase isolated from *F. solani pisi* corresponds to Gly32 (*11*), it was inferred that the first 31 amino acids constitute a transport peptide that is cleaved off (*9*). The 31 amino acids stretch was later suggested to be consisting of a 16 amino acids pre-sequence followed by a 15 amino acids pro-sequence (*12*, *13*). For bacterial recombinant expression, cutinase was N-terminally fused to the *Pho*A transport sequence to ensure transport to the periplasmic space. This construct still contained the 15 amino acids pro-sequence in order to allow proper cleavage of the *Pho*A peptide (*4*). The amino acid numbering used in the structure determination (*14*) was based on the protein carrying the additional N-terminal 15 amino acids pro-peptide. X-ray crystallographic data (*14*) as well as nuclear magnetic resonance (NMR)[1] assignments (*15*, *16*) showed that these 15 N-terminal amino acids constitute a very flexible region of the protein, which appears to be unstructured. A construct for fungal expression lacking the pro-peptide is also available (*12*). In this investigation, we use the 214 amino acid-long cutinase including these additional 15 amino acids.

Cutinase is a very well studied enzyme; a crystal structure with 1 Å resolution (*17*) and a complete assignment of its NMR resonances (*15*) are published. A number of investigations of the nature of the active site and its interaction with diverse substrates have been performed. Starting with the first X-ray investigation of the protein (*18*), it was discovered that cutinase has its catalytic serine exposed to the solvent, explaining why cutinase does not show interfacial activation (*14*). Later, a crystal structure of the protein inhibited by a substrate analogue was solved (*19*). Also, investigations of the intramolecular dynamics of cutinase with and without a phosphonate inhibitor have been reported (*16*, *20*).

The lack of interfacial activation has prompted for investigations of the environment surrounding the active site. The active site pocket is flanked by two loops. The definition

† This work has been supported by a grant from the Lundbeck Foundation (Denmark). R.W. acknowledges support by the Obel Foundation.

* To whom correspondence should be addressed. E-mail, rw@bio.aau.dk; tel, +45 96 35 85 18; fax, +45 98 14 18 08.

‡ Department of Physics and Nanotechnology, Aalborg University.

§ Department of Life Sciences, Aalborg University.

|| Present address: Novo Nordisk A/S, DK-3400 Hillerød, Denmark.

[1] Abbreviations: CMC, critical micelle concentration; DLS, dynamic light scattering; DOXYL, 4,4-dimethyloxazoline-*N*-oxyl; ESR (or EPR), electron spin resonance; HSQC, heteronuclear single-quantum coherence; MSG, mono stearic acid spin label glycerol; NMR, nuclear magnetic resonance; NOE, nuclear Overhauser effect; SASL, stearic acid spin label (DOXYL-stearic acid); TC4, (*R*)-1,2-dibutyl-carbamoylglycerol-3-*O*-*p*-nitrophenyl-butylphosphonate.

10.1021/bi060329i CCC: $33.50 
Published on Web 07/04/2006

of which amino acids belong to these loop regions has varied between the various investigations (*14*, *16*, *19*, *21*). All seem to include at least residues 80−87 and residues 180−188. The spanning of the loops defined in this investigation is based on the most recent definition (*16*) and includes residues 73−91 and residues 171−191.

The aim of this study is to investigate the interaction of cutinase with a lipid substrate and to detect the interaction of the enzyme with the substrate, as well as investigate the possibility of secondary interaction sites. To our knowledge, no data is currently available on the interaction of cutinase with a micellar glyceride substrate. A number of problems occur when trying to measure this interaction, the most obvious being that cutinase would catalyze the hydrolysis of the substrate during measurements at a rate which would exceed sampling rates for structural investigations. We have therefore chosen to work with the S120A cutinase mutant, which has previously been structurally characterized (*21*). Cutinase S120A shows a dramatically reduced catalytic rate of <0.06% compared to the wild-type using *p*-nitrophenylbutyrate as a substrate, and no activity could be detected on triacetin (unpublished data).

In protein engineering, it is often vital to map the regions of an enzyme where changes occur upon substrate interaction. NMR can provide such local information on enzymes with two parameters: chemical shifts and nuclear magnetic relaxation rates. Chemical shifts are very sensitive local probes for minute changes in the time-averaged chemical environment experienced by a nucleus. Nuclear magnetic relaxation provides one with the ability to investigate changes in intramolecular mobility upon changes in the chemical environment, for example, the addition of substrate to an enzyme.

In this work, we wanted to observe the changes in the enzyme molecule brought about by interaction with a substrate. Usually, the alkyl chains of fatty acids constituting the acyl-glycerol substrate do not exert, in their vicinity, a detectable influence on NMR signals. We chose to utilize spin-labeled fatty acid analogues, namely, 5- and 16-DOXYL-stearic acid (steric acid spin label, SASL) esterified to a glycerol backbone. Spin-labeled fatty acids carry a stable free radical. Such a free radical has a severe influence on the relaxation rates of the protein atoms in its vicinity. This is directly detectable by measuring the relaxation behavior of the groups of interest and is also evident in changes in signal strengths of heteronuclear single-quatum coherence (HSQC) spectra (*22*). Relaxation measurements are lengthy experiments; the experiments performed here typically take 14 days of experimental time. It is therefore of extreme importance to establish sample conditions under which the physicochemical properties of the lipid/water mixture do not change over a long time. Attempts to obtain stable micellar solutions with triacylglycerols failed. However, monoacylglycerols (mixtures of *sn*-1, *sn*-2, and *sn*-3) of both 5- and 16-DOXYL stearic acids (mono steric acid spin label glycerol, MSG) (Figure 1) proved to be stable in buffer at pH 7.

Here, we report changes in *F. solani pisi* cutinase upon interaction with monoacylglycerols of both 5- and 16-DOXYL stearic acid (Figure 1) in solution.

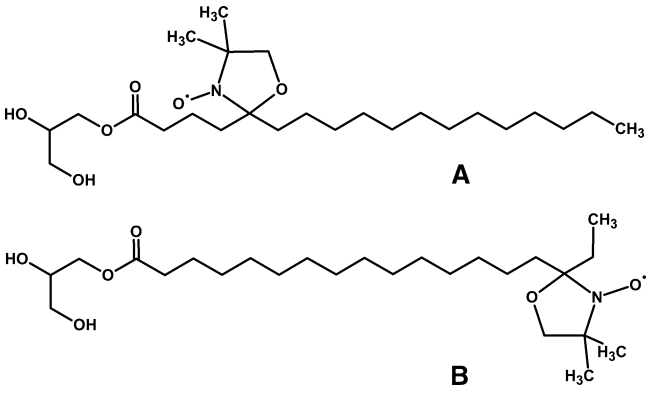


FIGURE 1: The structure of 5-DOXYL stearic acid (A) and 16-DOXYL stearic acid esterified to glycerol (B).

## EXPERIMENTAL PROCEDURES

*Plasmid Design.* The mutation S120A was obtained by site-directed mutagenesis using a Transformer Site-directed Mutagenesis Kit (Clonetech Laboratories, Inc.) where the primer was 5′-CGGTGGCTAC**GCT**CAGGTGCTG-3′. For expression purposes, the mutated gene was cloned, using the NdeI/BamHI restriction sites, into a pET11a (Novagen), generating the plasmid pFCEX1/S120A. Construction of the pFCEX1 plasmid is described in ref *23*.

*Production of Cutinase.* Production of cutinase S120A was performed in *Escherichia coli* BL21(DE3), having pFCEX1/S120A, in minimal medium (M9) containing uniformly labeled $^{13}C$ glucose and $^{15}N$ ammonium sulfate (99%, Spectra Stable Isotopes). The production and subsequent purification was carried out according to ref *24*.

*Production of SASL Monoglycerides (MSG).* Two varieties of MSG were synthesized from glycerol (99+% pure from Sigma Aldrich) and 5-DOXYL-stearic acid or 16-DOXYL-stearic acid (97% pure from Sigma Aldrich), respectively. The esterification reaction was carried out enzymatically using immobilized lipase from *Candida antarctica* (Novozyme 435 obtained from Novozymes, Denmark). A total of 5 mg of SASL was dissolved in 50 mL of *n*-hexane (95% from Sigma Aldrich), and a 10 times molar excess of glycerol and 10 mg of immobilized enzyme were added. The mixture was gently refluxed, to accelerate the reaction as well as to stir the mixture. The mixture was refluxed for 24 h for the 16-MSG and for 48 h for the 5-MSG. We attribute the longer reaction time needed for esterification of 5-SASL to the sterical hindrance of the DOXYL group which is situated closer to the carboxyl acid group. After stopping the reaction, the mixture was filtrated to remove the immobilized lipase, and the solvent was evaporated. The residual oily fraction was resuspended in chloroform, and the remaining nonreacted glycerol was removed by extracting the mixture with water. Verification of the formation of MSG was done using NMR. ESR was used to verify the presence of free radicals.

*NMR Measurements.* All NMR measurements were carried out using a Bruker DRX600 NMR spectrometer with a triple-axis gradient TXI (H/C/N) probe at 298 K. All NMR data were processed using XwinNMR3.6 and analyzed with the NEASY (*25*) tool of CARA (*26*). Samples for measuring the interaction of cutinase S120A with MSG were prepared by mixing 10 mg of uniformly labeled $^{13}C^{15}N$ S120A with the prepared MSG in 600 $\mu$L of phosphate buffer, pH 7, containing 5% $D_2O$ (99% Cambridge isotope labs) and 5

mM $NaN_3$. The sample was sonicated for 5 min (Elma Transonic Digital) to create the micellar solution, and larger lipid bodies were removed by low *g* centrifugation (60−80*g*). The final sample concentration was analyzed by FTIR, and micelle sizes were evaluated by DLS. The micellar solution was found to be stable for more than 4 weeks. Visual inspection did not indicate any signs of phase separation, that is, loss of micelles. This was corroborated by NMR measurements that do not exhibit any changes in the spectra even after several months of storage and after freezing/thawing. Moreover, ESR showed that the free radical was still present, even after extended periods of storage (>5 months). The reference sample of cutinase S120A was prepared by dissolving 10 mg of uniformly labeled $^{13}C^{15}N$ cutinase S120A in phosphate buffer, pH 7, containing 5% $D_2O$ and 5 mM $NaN_3$.

*Characterization of MSG Micellar Solutions by FT-IR and DLS.* The final concentration of MSG in the sample was determined by ATR-FTIR measurements on a Bruker IFS 66V/S spectrometer. A total of 10 $\mu$L of the final cutinase/lipid interaction sample was extracted with 500 $\mu$L of chloroform (99.9%+ Sigma), and chloroform was evaporated leaving the MSG. The MSG was dissolved in 20 $\mu$L of toluene (99.9%+ Sigma), and 2 $\mu$g of octadecylsilane (97% Sigma) was added as an internal standard. This was then compared to standard curves using both nonanoic acid (free fatty acid, 97% Sigma) and 1-monooleoyl-*rac*-glycerol (99% Sigma). The sizes of the lipid micelles were characterized by DLS using a Postnova analytics instrument with a PDDLS/CoolBatch 90T detector. DLS measurements were carried out on the NMR samples containing both cutinase and MSG.

*NMR Measurements.* To precisely determine chemical shift changes from the reference to the interaction sample, both $^{13}C$ decoupled $^{15}N^1H$-HSQC spectra (*27*) and 3D-HNCA (*28*) spectra were acquired. Apart from providing $C^\alpha$ chemical shifts, HNCA spectra were used for sequential assignment of those regions of the protein where the changes in the chemical shift of the signals upon interaction with substrate made a safe assignment based on the reference spectrum impossible. The HSQC spectra were acquired using 4 scans with 4 K and 512 complex data points and a spectral width of 13 and 40 ppm in the direct and indirect dimension, respectively. The HNCA data was obtained using 32 scans with 2 K complex data points and a spectral width of 13 ppm in the $^1H$ dimension, 24 complex data points and a spectral width of 40 ppm in the $^{15}N$ dimension, and 64 complex data points and a spectral width of 40 ppm in the $^{13}C^\alpha$ dimension. The $^{15}N$ $T_1$ and $T_2$ relaxation rate measurements (*29*) were acquired as pseudo-3D spectra using the standard Bruker interleaved pulse sequences. Delay times were 0.02, 0.1, 0.2, 0.4, 0.8, 1.6, and 5 s for the $T_1$ and 0, 16, 32, 48, 64, 80, 96, and 144 ms for the $T_2$ determination. For the $^1H^N$ $T_1$ relaxation rates, a modified version of the HSQC spectrum (*27*) was used incorporating an inversion recovery element (a 180° pulse on $^1H$ followed by a variable delay) prior to the HSQC pulse program. The data were obtained with delay times of 0.01, 0.05, 0.15, 0.5, 0.9, 1.6, and 7 s. $\{^1H\}$-$^{15}N$-NOE data (*29*) were collected with 72 scans using the standard Bruker interleaved pulse program with 5 s of irradiation on $^1H$ and a 3-9-19 water suppression scheme in the reverse INEPT step prior to acquisition. The relaxation rate of aliphatic $^1H^C$ was determined by incorporating an inversion recovery element prior to the existing $^{13}C^1H$-HSQC pulse program. The delays used were 0.0001, 0.02, 0.1, 0.4, 1, 2, and 5 s. The DOXYL group of 16-MSG was reduced by adding ascorbic acid to a final concentration of 80 mM and storing the sample at room temperature for 96 h. Afterward, relaxation rates of aliphatic $^1H^C$ were recorded as previously, with delays of 0.0001, 0.1, 0.4, 1, and 5 s.

*ESR Measurements.* Spectra were recorded on a Bruker EMX (Bruker, Rheinstetten, Germany) at room temperature. The microwave power was 20 mW, and a modulation frequency of 100 kHz with an amplitude of 0.5 G was used. The conversion time and time constant were both 20.48 ms.

## RESULTS

*Assignment of the S120A Mutant.* The X-ray structure of the cutinase S120A mutant has previously been published (*21*), but to our knowledge, no information on the NMR assignment has been reported. As the S120A mutation is responsible for significant shifts in the $^{15}N^1H$-HSQC spectrum, it was necessary to make a new assignment of parts of the backbone signals using HSQC and HNCA data, as well as building on the original NMR assignment data of the wild-type (*15*). The resulting assignment of S120A cutinase contains data for backbone $H^N$ (98%), N (98%), and $C^\alpha$ (98%) with $H^N$-N of amino acids 50, 87, 88, and 89 missing. For visualization, the changes are plotted on the published 3D structure of wild-type cutinase (PDB code 1CEX) (*17*). The wild-type structure was chosen because of its better resolution of 1 Å, rather than the published structure of the S120A mutant (PDB code 1CUI) (*21*) at 2.7 Å resolution. The changes plotted on the 1CEX structure can be seen in Figure 2; the observed chemical shift changes are mainly seen in and around the active site of cutinase, with the largest changes found in the loop regions and, as expected, at the site of the mutation.

*Sample Characterization.* The produced MSG is essentially of the 1-monoacylglycerol type, but it is well-known that acyl migration takes place (*30*), giving an equilibrium distribution of 1- and 2-monoacylglycerol with 88% of the *sn*-1-isomer and 12% of the *sn*-2- isomer (*31*). Using FT-IR, the final interaction sample was found to contain 2 mM 5-MSG and 1.8 mM 16-MSG, respectively. DLS yielded a hydrodynamic radius of the lipid aggregates of 4.3 nm.

*Interaction with MSG.* The signal-to-noise ratio in the HSQC spectra of the samples containing MSG was approximately 50−60% of its value in the spectra taken prior to addition of MSG. Since $^{15}N$-$R_1$ and -$R_2$ did not change for most residues, this is not a consequence of line broadening, but attributed to a loss of protein during sample preparation, most probably in the centrifugation step employed to remove large lipid aggregates.

The interaction of cutinase S120A with both the 5- and 16-MSG resulted in significant chemical shift changes for approximately 20% of the residues. Their backbone signals were reassigned using HSQC and HNCA spectra. In the presence of 5-MSG, the degrees of assignment obtained are $H^N$ (96%), N (96%), and $C^\alpha$ (96%) with 194 $H^N$-N pairs assigned (amino acids 42, 43, 50, 87, 88, 89, 121, 177, 194 missing). In presence of 16-MSG, the degrees of assignment

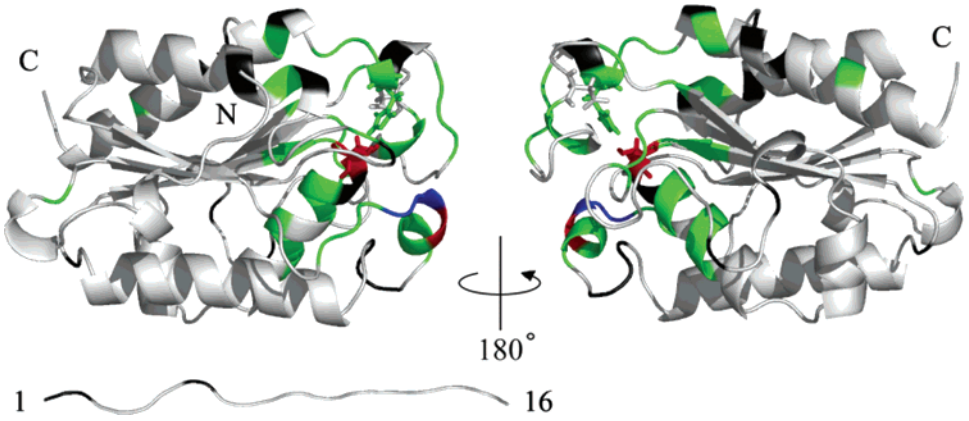


FIGURE 2: Mapping on a 3D graphic representation of the calculated chemical shift changes between WT cutinase and S120A mutant. Colors are black, no assignment; white, $\Delta\delta < 0.1$ ppm; green, $0.1 < \Delta\delta < 0.4$ ppm; blue, $0.4 < \Delta\delta < 0.8$ ppm; and red, $0.8 < \Delta\delta$ ppm. $\Delta\delta$ is calculated as $\Delta\delta = \sqrt{\Delta\delta_H^2 + (\Delta\delta_N/5)^2}$. The N-terminal flexible tail is represented by a strand of 16 amino acids at the bottom of the picture. The structure used is 1CEX (*17*).

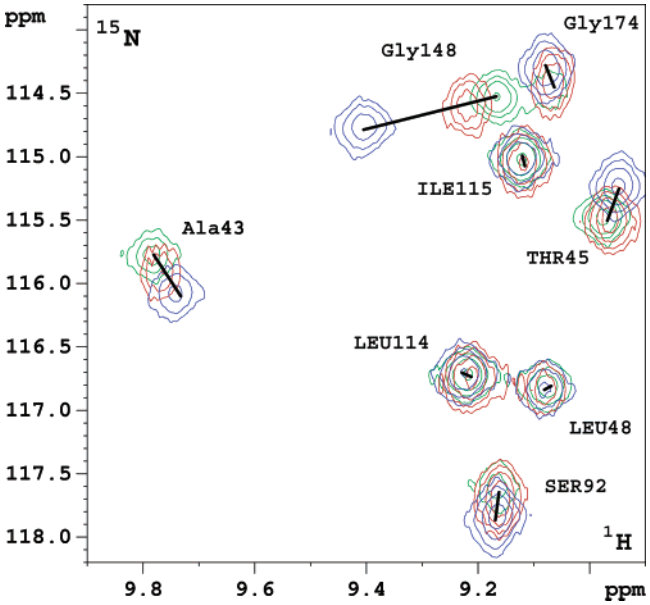


FIGURE 3: Changes in chemical shifts in a region of cutinase S120A HSQC spectrum upon addition of MSG. Green, no 5-MSG added; Red, 1 mM of 5-MSG; blue, 2mM of 5-MSG.

are $H^N$ (95%), N (95%), and $C^\alpha$ (95%), with 193 $H^N$-N pairs assigned (amino acids 32, 42, 43, 50, 87, 88, 89, 121, 151, 194 missing). An example of the observed changes in chemical shift can be seen in Figure 3, showing the change in chemical shift with increasing 5-MSG concentration. Figure 4 shows the chemical shift changes plotted on the 3D-structure of cutinase. The changes in chemical shift were found to mainly occur within the active site and loop regions. The magnitude and location of chemical shift changes upon interaction with 5-MSG and 16-MSG are essentially identical.

*Changes in the Relaxation Behavior of Cutinase upon Interaction with MSG.* Both the presence of substrate itself and the presence of a DOXYL radical in the substrate are expected to modulate the relaxation parameters of the S120A cutinase. The effect is twofold: changes in local and overall mobility will alter relaxation times, and the presence of the free radical will enhance nuclear magnetic relaxation in its proximity. $^{15}$N-$T_1$ and -$T_2$, $^1H^N$-$T_1$, and $^1H^C$-$T_1$ relaxation times as well as the $\{^1H\}$-$^{15}$N NOE were measured to detect changes in the relaxation behavior of the protein upon interaction with the spin-labeled monoacylglycerol. Throughout this paper, changes in NMR parameters occurring upon interaction with the lipid will be presented as

$$\Delta X = X_{\text{interaction}} - X_{\text{reference}} \quad (1)$$

where $X$ is the parameter in question and the subscript "interaction" defines the parameter obtained in the presence of MSG, while the subscript "reference" defines the parameter obtained in the absence of MSG.

The observed changes in relaxation behavior are summarized in Figures 5 and 6. Data obtained for $\Delta R_{1,N}$ and $\Delta R_{2,N}$ reveal only minute changes throughout the folded domain of the protein. In the mobile N-terminal tail region, changes in $^{15}$N relaxation behavior can be observed. On the basis of the average $R_2/R_1$ ratio of the $^{15}$N backbone atoms of the structured parts of cutinase, the cutinase molecule has a correlation time for overall tumbling, $\tau_m$, of 18.3 ns. This is somewhat higher than the 10.8 ns previously reported in the literature (*16*). Differing sample conditions, especially pH and ionic strength, can influence this value. The values previously reported were measured at pH 5 in a 10 mM acetate buffer (*16*). Changes observed in the $\{^1H\}$-$^{15}$N-NOE upon interaction with MSG are shown in the Supporting Information.

More changes upon addition of MSG were observed in $H^N$ relaxation: large negative $\Delta R_{1,HN}$ values are seen in the edges of the loop regions and, somewhat unexpected, also in the end of the N-terminal tail. The $\Delta R_{1,HN}$ data are plotted on the 3D-structure in Figure 7.

Relaxation rate changes of aliphatic protons ($\Delta R_{1,ali}$) reveal a group of atoms that relax significantly faster upon addition of 16-MSG. These data are visualized in Figure 8. A corresponding effect could not be seen upon addition of 5-MSG. To verify, that the observed relaxation enhancements originate from the DOXYL radical, relaxation rate changes of aliphatic protons were remeasured after reducing the DOXYL group with ascorbic acid. This resulted in a complete removal of relaxation enhancements as seen in Figure 6.

*ESR.* To verify the presence of the DOXYL radical during the NMR data acquisition, an ESR spectrum was recorded afterward, and as a reference, a sample of the pure

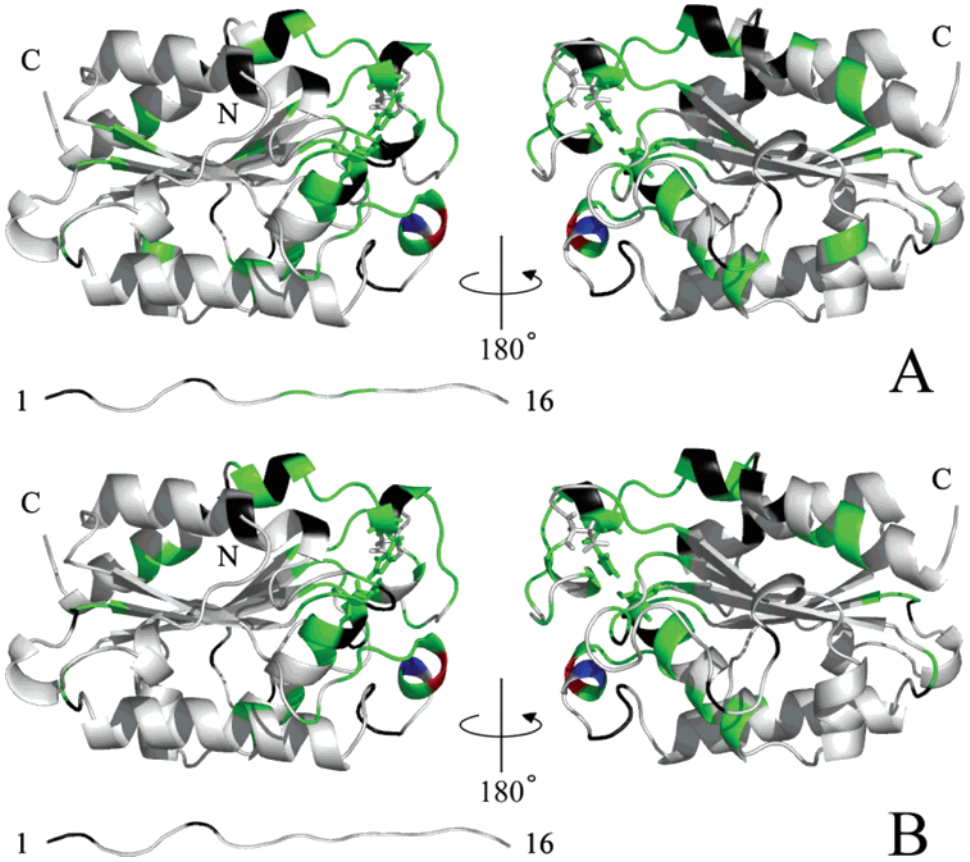


FIGURE 4: Mapping on a 3D graphic representation of the calculated chemical shift changes observed upon addition of (A) 5-MSG and (B) 16-MSG. Colors are black, no assignment; white, $\Delta\delta < 0.1$ ppm; green, $0.1 < \Delta\delta < 0.4$ ppm; blue, $0.4 < \Delta\delta < 0.8$ ppm; and red, $0.8 < \Delta\delta$ ppm. $\Delta\delta$ is calculated as $\Delta\delta = \sqrt{\Delta\delta_H^2 + (\Delta\delta_N/5)^2}$. The N-terminal flexible tail is represented by a strand of 16 amino acids at the bottom of the picture. The structure used is 1CEX (*17*).

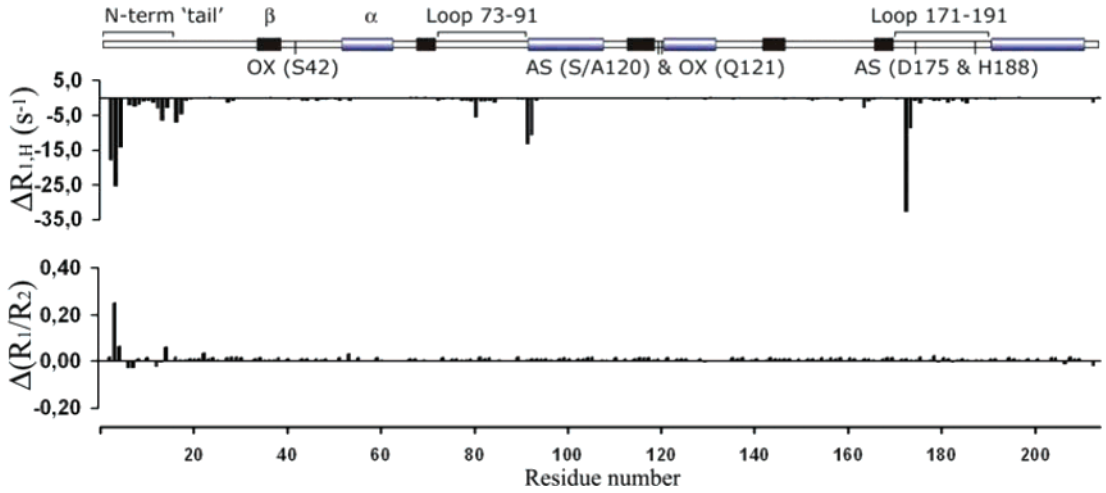


FIGURE 5: Measured changes in the $H^N$ longitudinal relaxation rates ($\Delta R_{1,H}$, estimated uncertainty $\pm 0.5$ $s^{-1}$) and N $R_1/R_2$ relaxation rates ($\Delta R_1/R_2$, estimated uncertainty $\pm 0.08$) upon addition of 5-MSG. Changes represented as a difference: $\Delta$ = interaction − reference. The cutinase sequence is represented schematically on top of the graphs, with α-helices and $\beta$-strands as blue and black boxes, respectively. Active site residues are marked with vertical bars. AS, active site; OX, oxyanion hole.

5-DOXYL-stearic acid was also measured. All NMR samples showed the presence of the DOXYL radical after NMR acquisition (data not shown).

## DISCUSSION

*S120A versus WT Cutinase.* The S120A cutinase mutant was employed in this study in order to characterize interactions between the protein and monoglyceride substrates. As no NMR assignment was available for this mutant, we undertook a comparison between the active WT cutinase and the inactive S120A mutant. Overall, no evidence for a change in structure was found by introducing the mutation, as the detected changes in chemical shift were <0.05 ppm for H and <0.1 ppm for N for all backbone $N^H$ pairs, except for the $N^H$ pairs in close vicinity to the S120A mutation. The largest chemical shift changes occurred at the mutation site

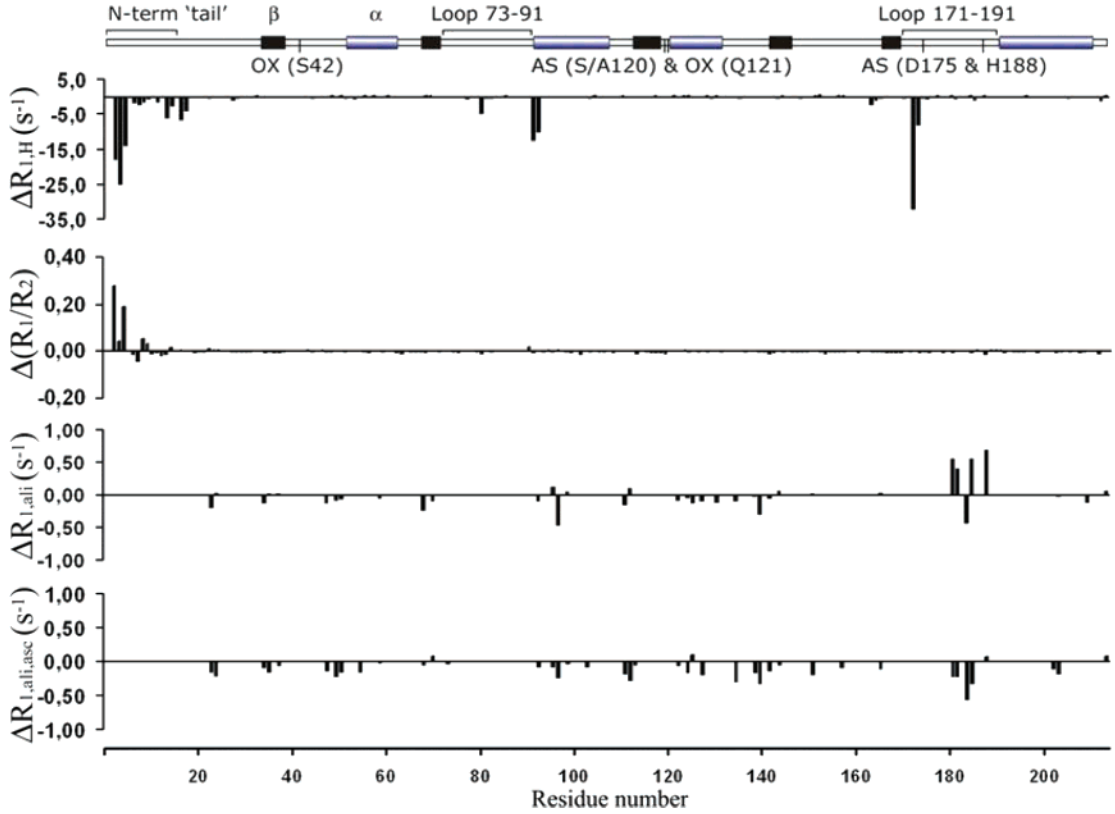


FIGURE 6: Measured changes in relaxation rates upon addition of 16-MSG. $H^N$ longitudinal relaxation ($\Delta R_{1,H}$, estimated uncertainty $\pm 0.65$ $s^{-1}$), N $R_1/R_2$ relaxation rates ($\Delta R_1/R_2$, estimated uncertainty $\pm 0.09$), longitudinal relaxation rates from aliphatic side-chain protons before ($\Delta R_{1,ali}$, estimated uncertainty $\pm 0.09$ $s^{-1}$) and after ($\Delta R_{1,ali,asc}$, estimated uncertainty $\pm 0.12$ $s^{-1}$) reduction of the DOXYL radical by ascorbic acid. Changes represented as a difference: $\Delta$ = interaction − reference. The cutinase sequence is represented schematically on top of the graphs, with α-helices and *β*-strands as blue and black boxes, respectively. Active site residues are marked with vertical bars. AS, active site; OX, oxyanion hole.

and in the loop region immediately adjacent to the S120A mutation in space (Ala79−Asn84) (Figure 2). This indicates that the change brought about by the S120A mutation had little or no influence on the actual structure of the protein. The published X-ray structure of S120A cutinase (*21*) also indicates that the mutant structure is unaltered under crystallization conditions. This leads to the conclusion that cutinase S120A only shows slight structural changes. The observed changes in chemical shift stem from changes in the chemical environment caused by the removal of the Ser120-OH group.

*On the Interpretation of NMR Data.* When a protein is interacting with a substrate or a ligand, many effects come into play, which make this event detectable by NMR. The substrate will bind to the active site pocket of the enzyme, and this binding will alter the structure of the active site to some extent and change the mobility or freedom of motion. Mobility changes can occur on the level of single amino acids, stretches of amino acids, or the whole protein molecule.

Several NMR tools are available to describe these changes; the simplest is to look for changes in the chemical shifts, as the chemical shift for any given atom in the protein is given by its chemical environment. Therefore, any change in the local structure of a protein will yield a change in the chemical shift of nearby atoms. However, chemical shift changes do not contain information about the nature of these changes.

The information extracted from the various relaxation data can be divided into three groups: overall molecular motion, internal dynamics, and vicinity to the DOXYL moiety.

$^{15}N$ backbone relaxation measurements are used for the determination of the overall mobility. The common method for measuring mobility on the amino acid scale is the $\{^1H\}$-$^{15}N$ NOE. NOEs are dependent on the mobility of the atoms involved and are therefore a useful tool in describing local mobility. In the case of cutinase, their use is, however, limited to very flexible regions of the molecule, such as the tail region. Changes in intramolecular mobility of regions with moderate flexibility can best be detected by $^1H$-relaxation, since $^{15}N$-relaxation is not sensitive enough in this particular motional regime. $\{^1H\}$-$^{15}N$ NOE changes of cutinase upon interaction with 5- and 16- MSG were collected. They did not show any significant changes compared to the reference, and are available as Supporting Information.

To correctly interpret the changes in the measured relaxation parameters, it is possible to simulate how they depend on the correlation time, based on the equations given by ref *32*.

In addition, the MSG used here also carries a stable free radical in the form of a DOXYL spin label. Free radicals have the effect of enhancing relaxation. This effect is distance-dependent, and therefore, only atoms close to the DOXYL group will show the effect.

*Cutinase Interacts Weakly with the Lipid Micelles.* The chemical shift changes occurring upon addition of lipids to the protein solution appear to be concentration-dependent at concentrations above the cmc (Figure 3). This is taken as evidence that the observed changes indeed stem from an

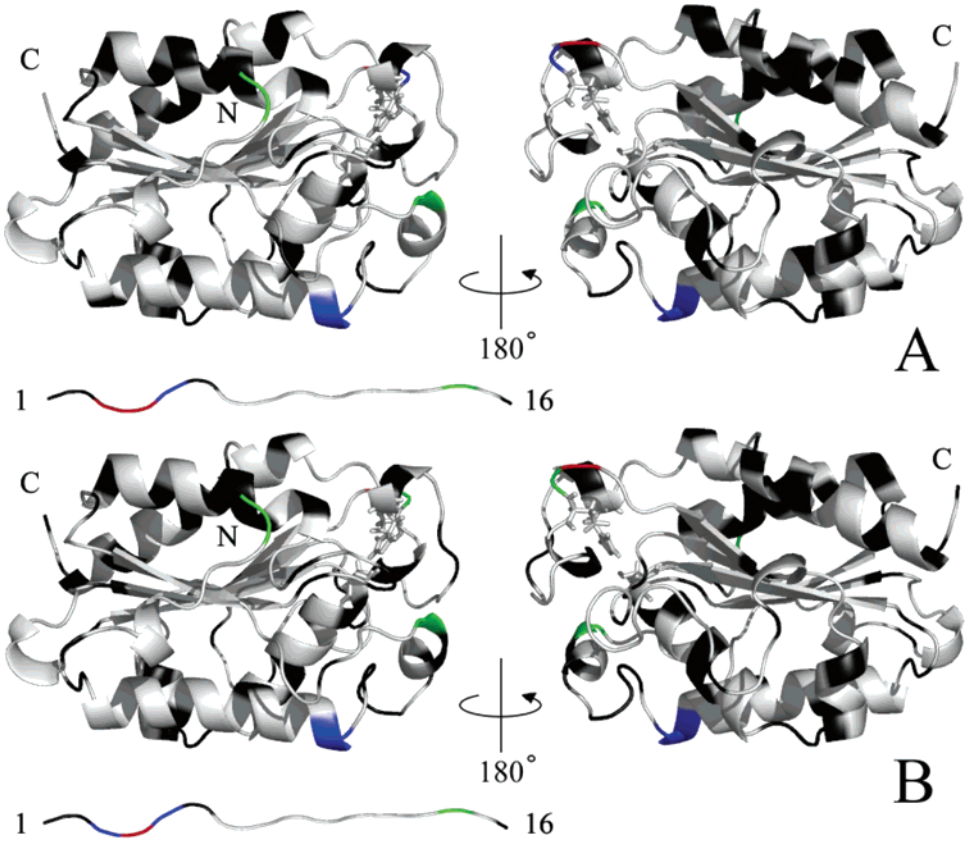


FIGURE 7: Mapping on a 3D graphic representation of the measured changes in the $H^N$ longitudinal relaxation rates upon addition of (A) 5-MSG and (B) 16-MSG. Colors are black, either proline residues or no assignment or no reliable relaxation rate can be measured due to spectral overlap; white, $\Delta R_{1,H} > -3\ s^{-1}$; green, $-3 > \Delta R_{1,H} > -8\ s^{-1}$; blue, $-8 > \Delta R_{1,H} > -16\ s^{-1}$; and red, $-16 > \Delta R_{1,H}\ s^{-1}$.

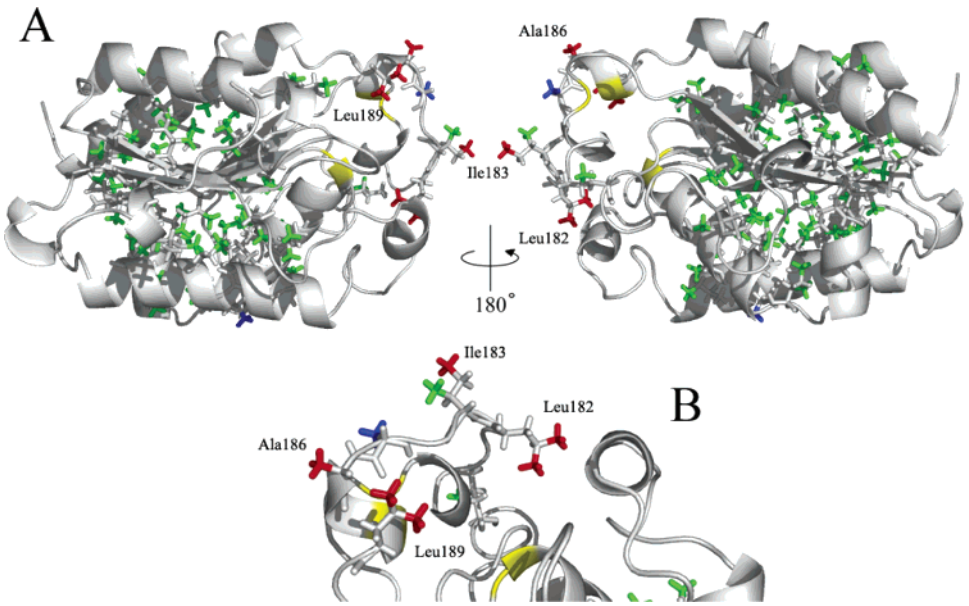


FIGURE 8: Mapping of the changes in longitudinal relaxation rates from aliphatic side-chain protons ($\Delta R_{1,ali}$) upon addition of 16-MSG on the structure 1CEX (*17*). All methyl groups for which relaxation rates could be measured are shown in stick structure, with a detected change of $\Delta R_{1,ali} > 0.3\ s^{-1}$ shown in red, $\Delta R_{1,ali} < -0.3\ s^{-1}$ shown in blue, and $-0.3 < \Delta R_{1,ali} < 0.3\ s^{-1}$ shown in green. The active site amino acids are colored in yellow. (A) All detected changes and (B) close-up of the active site region.

interaction of the protein with the lipid micelles. However, a strong binding of the cutinase molecule to the micellar surface can be ruled out based on the $^{15}N$-$R_1$ and -$R_2$ relaxation rates. The binding of a protein molecule to a larger particle (e.g., a micelle) will result in an increased $\tau_m$, which in turn will result in an increasing $R_2/R_1$ ratio. As this was not observed, it is concluded that the interaction of cutinase with the micelles is weak, and the association equilibrium is shifted toward the free enzyme molecule under our measurement conditions. However, during preparation of the protein/lipid sample, approximately 50% of the protein NMR signals were lost in a step involving centrifugation of large lipid aggregates. This indicates a significantly stronger interaction of the protein with these large aggregates.

*The Interaction between Cutinase and the Substrate Takes Place around the Active Site.* The observed chemical shift changes upon lipid interaction are well in line with changes observed previously upon covalent binding of (*R*)-1,2-dibutyl-carbamoylglycerol-3-*O*-*p*-nitrophenyl-butylphosphonate (TC4) (*20*). Changes upon interaction larger than 0.1 ppm in $^{1}$H and/or 0.2 ppm in $^{15}$N are found in the two loop regions flanking the active site and the region around Ser 42 of the oxyanion hole, suggesting that at least some rearrangement is occurring in this region of the protein. The oxyanion hole was reported to be preformed based on the original X-ray structure (*1*, *14*); later NMR investigations showed that the oxyanion hole had some flexibility in solution and that this mobility was lost when binding to an inhibitor (*16*, *20*). Chemical shift changes are low throughout the rest of the protein molecule. This leads to the conclusion that cutinase S120A mutant interacts with the substrate through the entrance of its active site pocket, as no chemical shift changes are detected on the rest of the surface. Thus, no evidence for any secondary interaction site in the folded domain of cutinase has been found. In addition, there is also evidence that the bottom of the active site cavity is occupied by the substrate. Thus, we conclude that cutinase S120A interacts in the same way as the active wild-type protein would, even though S120A is lacking the ability to form the covalent ES complex.

*Expected and Unexpected Mobility Changes upon Micelle Interaction.* The data obtained for $\Delta R_{1,H}$ show three distinct regions for which relaxation properties change significantly. Two of these are located in the loops flanking the active site. Ser 92, Ala 93, Thr 173, and Gly 174 show the greatest changes upon interaction; both amino acid pairs are positioned at the edge of the loop regions, indicating that they might act as a kind of hinges during the interaction, allowing for the loops to move. On the basis of our own relaxation data and data reported elsewhere (*20*), the effective correlation time for cutinase backbone atoms of the folded domain is in the limit, where a decreasing $R_1$ corresponds to decreasing molecular mobility. The loops surrounding the active site are becoming less flexible upon interaction with the lipid micelle. This decrease in mobility of the loop regions was also found when cutinase was covalently bound to an inhibitor (*20*).

An interesting and somewhat unexpected finding is that also Thr 3, Ser 4, Asn 5, and to some extent all amino acids up to Thr 18 show a large change in relaxation behavior. This strongly indicates that the tail region of cutinase is in one way or another affected by the presence of the lipid. The first 15 N-terminal amino acids of the cutinase used in the present study are a remnant of a 31 amino acid pre-propeptide and are, as such, not of prime interest. Nevertheless, in the literature, both this particular variant of cutinase as well as a variant devoid of this N-terminal stretch of 15 amino acids have been used, and there seems to be no consensus on its significance (or lack thereof). We show here that the N-terminal tail becomes less flexible by the binding of cutinase to a monoacylglycerol substrate. There is no evidence for any role of the tail residues in substrate interaction. Probably, the random movement of the tail is restricted to a smaller volume when cutinase binds to the substrate, resulting in the observed lower mobility.

The fact that no significant differences are found in the backbone relaxation data between the 5- and 16- MSG suggests that the glycerol moiety is responsible for the main part of the changes observed.

*Hydrophobic Residues Surrounding the Active Site Are Found To Interact with the Fatty Acid.* The $\Delta R_{1,ali}$ only contains data for a limited number of atoms due to considerable overlap in this region of the spectrum. In particular, we lack data from the N-terminal tail, as these signals are all placed in crowded regions of the spectra. The $\Delta R_{1,ali}$ is the only data exhibiting the expected increase in relaxation rates from the interaction with the DOXYL radical. Theoretically, this enhanced relaxation rate could also stem from increased molecular mobility upon protein substrate interaction. However, this is clearly not the case, as relaxation enhancements vanish upon reduction of the DOXYL group by ascorbic acid, for some amino acids even turning into a relaxation decrease, showing that the mobility of the loop in fact is decreased. As seen in Figure 8, only residues in one of the loops next to the active site of cutinase exhibit enhanced relaxation. In particular, the atoms Leu182 ($C^{\delta}/H^{\delta}$), Ile183 ($C^{\delta 1}/H^{\delta 1}$), Ala186 ($C^{\beta}/H^{\beta}$), and Leu189 ($C^{\delta}/H^{\delta}$) show an increasing relaxation rate. It must be noted that the Leu $C^{\delta}/H^{\delta}$ pairs are not stereospecifically assigned in the published NMR assignment; thus, we do not know which of the two methyl groups is affected. Looking at Figure 8B, we see that the involved atoms are those protruding the furthest from the protein surface. A previous study (*19*) reported that Leu189 ($C^{\delta}/H^{\delta}$) directly interacts with TC4 (covalently bound inhibitor) and that residues 182, 183, 186, and 189 all have a contact surface larger than 10 Å$^2$ with TC4. Another study with TC4 (*20*) also pointed at residues 183 and 189 to be involved in the interaction. This study also reported altered mobility of the loop from residue 171−191.

Remarkably, only aliphatic methyl protons showed increased relaxation rates upon interaction with the DOXYL moiety, while not a single case of relaxation enhancement has been found for backbone $H^N$ atoms. This is attributed to the fact that the relaxation enhancement is distance-dependent and the effect on atoms on the surface of the protein is therefore stronger than the effect on backbone atoms. Overall, the effect is very weak here, because the interaction between the protein and the lipid is quite weak, with its equilibrium shifted toward free cutinase.

## CONCLUSION

From the data presented above, it is possible to infer a picture of the substrate interaction of cutinase. In solution, cutinase maintains mostly a rigid structure with some flexible elements, essentially the N-terminal tail and the two loops flanking the active site. The flexibility of the active site loops is likely to make it possible for cutinase to have an activity toward water-soluble esters. When cutinase is presented with MSG micelles, it will loosely interact with their surface. No direct evidence for an additional binding site was found in this study. However, we observe mobility changes in the tail region of the protein, distant from the active site, upon interaction with the lipid. Interaction with the micelles also results in a rearrangement of the active site loops and a lowered mobility of the loop regions. The fact that this mobility change is most predominant at the edge or anchor

point of the loop region supports the idea of a "mini-lid" or "flap helix" and the need for some structural rearrangement upon substrate binding as suggested by Prompers et al. (*20*).

Spin-labeled lipids were shown to be a valuable means of obtaining information on the interaction between esterases and their substrates in solution.

## ACKNOWLEDGMENT

The authors thank Lars Haastrup Pedersen for providing immobilized lipase from *Candida antarctica*, Lars Duelund for being instrumental in getting the much appreciated ESR data, Lise Giehm for help with the DLS equipment, and Norbert Müller for valuable discussions.

## SUPPORTING INFORMATION AVAILABLE

Chemical shift changes and changes in $\{^1H\}$-$^{15}N$ NOE. This material is available free of charge via the Internet at http://pubs.acs.org.

## REFERENCES

1. Martinez, C., Nicolas, A., van Tilbeurgh, H., Egloff, M. P., Cudrey, C., Verger, R., and Cambillau, C. (1994) Cutinase, a lipolytic enzyme with a preformed oxyanion hole, *Biochemistry 33*, 83−89.
2. Schrag, J. D., and Cygler, M. (1997) Lipases and alpha/beta hydrolase fold, *Methods Enzymol. 284*, 85−107.
3. Chahinian, H., Nini, L., Boitard, E., Dubes, J. P., Comeau, L. C., and Sarda, L. (2002) Distinction between esterases and lipases: a kinetic study with vinyl esters and TAG, *Lipids 37*, 653−662.
4. Lauwereys, M., De Geus, P., De Meutter, J., Stanssens, P., and Mathyssens, G. (1991) Cloning, expression and characterization of cutinase, a fungal lipolytic enzyme, in *Lipases—Structure, Function and Genetic Engeneering* (Alberhina, L., Schmid, R. D., and Verger, R., Eds.) pp 243−251, VCH, Weinheim, Germany.
5. Purdy, R. E., and Kolattukudy, P. E. (1973) Depolymerization of a hydroxy fatty acid biopolymer, cutin, by an extracellular enzyme from *Fusarium solani f. pisi*: isolation and some properties of the enzyme, *Arch. Biochem. Biophys. 159*, 61−69.
6. Kolattukudy, P. E. (1984) Cutinases from fungi and pollen, in *Lipases* (Borgsröm, B., and Brockman, H. L., Eds.) pp 472−504, Elsevier, Amsterdam, The Netherlands.
7. Purdy, R. E., and Kolattukudy, P. E. (1975) Hydrolysis of plant cuticle by plant pathogens. Properties of cutinase I, cutinase II, and a nonspecific esterase isolated from *Fusarium solani pisi*, *Biochemistry 14*, 2832−2840.
8. Purdy, R. E., and Kolattukudy, P. E. (1975) Hydrolysis of plant cuticle by plant pathogens. Purification, amino acid composition, and molecular weight of two isozymes of cutinase and a nonspecific esterase from *Fusarium solani f. pisi*, *Biochemistry 14*, 2824−2831.
9. Soliday, C. L., Flurkey, W. H., Okita, T. W., and Kolattukudy, P. E. (1984) Cloning and structure determination of cDNA far cutinase, an enzyme involved in fungal penetration of plants, *Proc. Natl. Acad. Sci. U.S.A. 81*, 3939−3943.
10. Soliday, C. L., Dickman, M. B., and Kolattukudy, P. E. (1989) Structure of the cutinase gene and detection of promoter activity in the 5′-flanking region by fungal transformation, *J. Bacteriol. 171*, 1942−1951.
11. Lin, T. S., and Kolattukudy, P. E. (1980) Structural studies on cutinase, a glycoprotein containing novel amino acids and glucuronic acid amide at the N terminus, *Eur. J. Biochem. 106*, 341−351.
12. van Gemeren, I. A., Musters, W., van den Hondel, C. A., and Verrips, C. T. (1995) Construction and heterologous expression of a synthetic copy of the cutinase cDNA from *Fusarium solani pisi*, *J. Biotechnol. 40*, 155−162.
13. van Gemeren, I. A., Beijersbergen, A., Musters, W., Gouka, R. J., van den Hondel, C. A., and Verrips, C. T. (1996) The effect of pre- and pro-sequences and multicopy integration on heterologous expression of the *Fusarium solani pisi* cutinase gene in *Aspergillus awamori*, *Appl. Microbiol. Biotechnol. 45*, 755−763.
14. Martinez, C., De Geus, P., Lauwereys, M., Matthyssens, G., and Cambillau, C. (1992) *Fusarium solani* cutinase is a lipolytic enzyme with a catalytic serine accessible to solvent, *Nature 356*, 615−618.
15. Prompers, J. J., Groenewegen, A., Van Schaik, R. C., Pepermans, H. A., and Hilbers, C. W. (1997) $^1H$, $^{13}C$, and $^{15}N$ resonance assignments of *Fusarium solani pisi* cutinase and preliminary features of the structure in solution, *Protein Sci. 6*, 2375−2384.
16. Prompers, J. J., Groenewegen, A., Hilbers, C. W., and Pepermans, H. A. (1999) Backbone dynamics of Fusarium solani pisi cutinase probed by nuclear magnetic resonance: the lack of interfacial activation revisited, *Biochemistry 38*, 5315−5327.
17. Longhi, S., Czjzek, M., Lamzin, V., Nicolas, A., and Cambillau, C. (1997) Atomic resolution (1.0 Å) crystal structure of *Fusarium solani* cutinase: stereochemical analysis, *J. Mol. Biol. 268*, 779−799.
18. Abergel, C., Martinez, C., Fontecilla-Camps, J., Cambillau, C., de Geus, P., and Lauwereys, M. (1990) Crystallization and preliminary X-ray study of a recombinant cutinase from *Fusarium solani pisi*, *J. Mol. Biol. 215*, 215−216.
19. Longhi, S., Mannesse, M., Verheij, H. M., De Haas, G. H., Egmond, M., Knoops-Mouthuy, E., and Cambillau, C. (1997) Crystal structure of cutinase covalently inhibited by a triglyceride analogue, *Protein Sci. 6*, 275−286.
20. Prompers, J. J., van Noorloos, B., Mannesse, M. L., Groenewegen, A., Egmond, M. R., Verheij, H. M., Hilbers, C. W., and Pepermans, H. A. (1999) NMR studies of *Fusarium solani pisi* cutinase in complex with phosphonate inhibitors, *Biochemistry 38*, 5982−5994.
21. Longhi, S., Nicolas, A., Creveld, L., Egmond, M., Verrips, C. T., de Vlieg, J., Martinez, C., and Cambillau, C. (1996) Dynamics of *Fusarium solani* cutinase investigated through structural comparison among different crystal forms of its variants, *Proteins 26*, 442−458.
22. Kosen, P. A. (1989) Spin labeling of proteins, *Methods Enzymol. 177*, 86−121.
23. Neves-Petersen, M. T., Petersen, E. I., Fojan, P., Noronha, M., Madsen, R. G., and Petersen, S. B. (2001) Engineering the pH-optimum of a triglyceride lipase: from predictions based on electrostatic computations to experimental results, *J. Biotechnol. 87*, 225−254.
24. Poulsen, K. R., Snabe, T., Petersen, E. I., Fojan, P., Neves-Petersen, M. T., Wimmer, R., and Petersen, S. B. (2005) Quantization of pH: Evidence for acidic activity of triglyceride lipases, *Biochemistry 44*, 11574−11580.
25. Bartels, C., Xia, T.-H., Billeter, M., Günter, P., and Wüthrich, K. (1995) The program XEASY for computer-supported NMR spectral analysis of biological macromolecules, *J. Biomol. NMR 5*, 1−10.
26. Keller, R. (2004) *The Computer Aided Resonance Assignment Tutorial*, Cantina Verlag, Goldau, Switzerland.
27. Mori, S., Abeygunawardana, C., Johnson, M. O., and van Zijl, P. C. (1995) Improved sensitivity of HSQC spectra of exchanging protons at short interscan delays using a new fast HSQC (FHSQC) detection scheme that avoids water saturation, *J. Magn. Reson., Ser. B 108*, 94−98.
28. Ikura, M., Kay, L. E., and Bax, A. (1990) A novel approach for sequential assignment of 1H, 13C, and 15N spectra of proteins: heteronuclear triple-resonance three-dimensional NMR spectroscopy. Application to calmodulin, *Biochemistry 29*, 4659−4667.
29. Farrow, N. A., Muhandiram, R., Singer, A. U., Pascal, S. M., Kay, C. M., Gish, G., Shoelson, S. E., Pawson, T., Forman-Kay, J. D., and Kay, L. E. (1994) Backbone dynamics of a free and phosphopeptide-complexed Src homology 2 domain studied by $^{15}N$ NMR relaxation, *Biochemistry 33*, 5984−6003.
30. Fischer, E. (1920) Wanderung von Acyl bei den Glyceriden, *Ber. Dtsch. Chem. Ges. 53*, 1621−1633.
31. Mattson, F. H., and Volpenhein, R. A. (1962) Synthesis and properties of glycerides, *J. Lipid Res. 3*, 281−296.
32. Kay, L. E., Torchia, D. A., and Bax, A. (1989) Backbone dynamics of proteins as studied by $^{15}N$ inverse detected heteronuclear NMR spectroscopy: Application to staphylococcal nuclease, *Biochemistry 28*, 8972−9.

BI060329I